**Thank you for your comments and suggestions, some modifications have been made in order to clarify the paper and highlight the contributions.**

**1. The novelty is not clear, a sentence on what is new would help**

Cameras are usually set at high-speed of recording, being necessary to reduce the spatial resolution in order to achieve this speed. In our case, the camera was set at full resolution. The small gap between frames was achieved through both a fast LED and set the camera to a PIV mode. This configuration was inspired by the PIV technique and it allows a time gap between frames of 2.5 μs at full frame, which is equivalent a recording speed of 400000 fps. Additionally, if it selects a reasonable resolution, it will impossible with the first configuration mentioned.

**The following paragraph was added:**

This proposed configuration allows the use of the full frame of the camera (2560 x 1600 pixels) and thus, obtain a high spatial resolution thanks to the recording speed was set a relatively low value, the quite small gap time between images is achieved through an ultra-fast LED suitably triggered.

**2. It is not clear what is the pixel size (resolution)**

**The following sentence was added:**

Infinity K2 DistaMax lens provided a spatial resolution of the images of 5.6 μm per pixel

**3. what is the experimental uncertainly because of that?**

Taking into account, the spatial resolution the error could be around 1 pixel but considering that the diameter was calculated integrating the intensity from at least 15 pixels, the error expected is likely lower. This considered error (1 pixel) in small particles leads to a high relative error which decreases with increasing the particle diameter. Currently, we are working on improving our optical setup to achieve a spatial resolution of up to 3 μm per pixel, which allows decreasing the error. Additionally, we expect to validate our results with a laser-technique such as PDPA as soon as possible.

**4. what is the overall experimental uncertainty if the various parameters measured?**

The particle velocity was calculated with respect to the movement of the centroid, taking into account that the centroid was calculated integrating at least 15 pixels, we can expect an error as a maximum of 0.1 pixels, that is sub-pixel accuracy. Furthermore, taking into account that a characteristic displacement of a droplet can be around 10 pixels, we would obtain an uncertainty of 1%.

**5. how well are the various experimental parameters controlled?**

Both size and velocity are influenced by the injection pressure and air surrounding flow which have a standard deviation of 0.8% and 0.45% respectively.

# Experimental study of the influence of the boundary conditions on the atomization process in an unconfined atmospheric burner

Raul Payri, Francisco J. Salvador, Jaime Gimeno, Santiago Cardona *
[1]CMT - Motores Térmicos, Camino de Vera (s/n), Universitat Politècnica de València, Edificio 6D, 46022, Valencia, Spain.
*Corresponding author: sancarv1@mot.upv.es

**Abstract**
The present work was realized in order to understand the influence of the boundary conditions on the atomization process in an atmospheric continuous-flow burner, which consists of an annular non-swirling co-flow of air that surrounds a central cone spray atomized by a commercial simplex injector. A new Microscopic diffused back-illumination (MDBI) technique was used to analyze droplet diameter and droplet velocity near to the injector outlet. The spray distribution yields small droplets along the spray-axis while the majority of the mass is situated as big droplets along the spray borders. Furthermore, a new test rig was designed to analyze the atomization and combustion phenomena in this sort of burners under different ambient conditions and geometrical setups, this facility is capable of reaching an air flow of $400\,\mathrm{kg/h}$ and air temperatures up to $673\,\mathrm{K}$ (depending on the air mass flow). The test matrix implemented consisted of a variation of injection pressure at fixed air surrounding conditions (mass flow and temperature) and an air outlet diameter of $21\,\mathrm{mm}$. The experiments were carried out with n-heptane, n-dodecane, and n-hexadecane. Physical properties of the fluid demonstrated to have a noteworthy influence on the global spray performance as well on the droplet velocity and droplet size near the nozzle exit.

**Keywords**
Simplex nozzle, MDBI, Spray Characteristics, Droplets.

## Introduction

Burners are being continuously improved in order to produce lower emissions and higher efficiency. This requires a fundamental understanding of the processes involved in two phase and lean combustion process. Additionally, spray combustion involves many complex physical phenomena, including atomization, dispersion, evaporation, and combustion, which generally take place simultaneously or within very small regions in the combustion chambers. Accurate experimental data are necessary to understand the fuel droplet interaction with the flame structure along evaporation and combustion steps, in this perspective of moving forward into more complex configurations (e.g., aeronautical, gas turbine, ...). Experimental investigations [1–3] are needed to promote or support of the numerical modeling works. Spray jet flame has been widely investigated including studies on the flame structure [4–7].

The atomization process has been largely studied using numerous optical techniques, mainly laser techniques. Friedman et al. [5] used Phase Doppler Interferometry (PDI) to measure fuel droplet size and velocity of the methanol spray in an annular air jet. PDI is based in the measuring of the phase difference and frequency of light scattered when a droplet passes through the intersection of two laser beams. Meanwhile, Marley et al. [6] employed Phase Doppler Anemometry (PDA) and Laser Doppler Velocimetry (LDV) to determine the spray dispersion and aerodynamic properties of an ethanol spray.

Currently, the experimental investigation of local flame structures and fuel droplet properties continuous using mainly high-speed diagnostics. A. Verdier et al. [8] investigated flow topology of n-heptane spray applying experimental techniques such as Phase Doppler Anemometry (PDA). Meanwhile, I. Düwel et al. [9] performed a combined experimental and numerical study of a spray burner, where air and liquid fuel are injected at ambient temperature favoring direct droplet interaction, both experiment and simulation are in very good agreement in terms of gas and liquid velocities profiles, and droplet size distribution. A. Verdier et al. [10] studied an n-heptane spray jet flame in an annular non-swirled air co-flow that surrounds a central hollow-cone spray injector through quantitative measurements using laser-based techniques. PDA measurements contributed to the analysis of air and droplet aerodynamics and Global Rainbow Refractometry Technique (GRT) was used to measure droplet temperature in the different regions of the spray jet. Finally, J. Marrero-Santiago et al. [11] implemented PDA also to measured droplet size-velocity in n-heptane spray, and High-speed Particle Image Velocimetry (PIV) to measure the instantaneous velocity fields.

The focus of this document is the description of microscopic characterization of the spray jet through an optical setup denoted as MDBI (microscopic diffused back-illumination), determining droplet diameter and velocity distribution. The methodology is based on the optical setup known as back-light in a far-field and near-field configuration, which has been widely used to study different parameters such as spray penetration, spray angle, and droplet size[12–16]. This proposed configuration allows the use of the full frame of the camera (2560 x 1600 pixels) and thus, obtain a high spatial resolution thanks to the recording speed was set a relatively low value, the quite small gap time between images is achieved through an ultra-fast LED suitably triggered. A flow test rig was designed which is able of

delivering hot air-flow at desired conditions of air mass flow and temperature and the burner has enough flexibility to evaluate different geometrical configurations.

The manuscript is divided into four sections. After the introduction, the experimental facility is described, along with the details of the optical configuration and the image processing implemented in this work. The results are presented and discussed next for the measured parameters. Finally, the conclusions obtained through the execution of this work are presented.

## Material and methods

This section explains the test rig used to carry out the study of the atomization process in continuous flow burners and optical technique. The installation is capable of reaching high air flow and temperature and it was developed in the facilities of CMT–Motores Térmicos in the Universitat Politècnica de Valencia. This test rig has a completely optical accesses that allow the use of different optical techniques which are explained in detail in the following subsections.

### *High flow and temperature installation for continuous burner*

Test rig employed to study the behavior of the atomization and combustion processes in continuous burners is presented in Figure 1. The installation is composed mainly by a centrifugal blower, two hot-wire flow meters, a 15 kW electric heater, an injection system, and a continuous flow burner. Additionally, it has multiples valves and pipelines to control the air flow, the test rig refrigeration, and seeding module. The installation can be operated in a wide range of operation conditions, allowing the study of the spray atomization and combustion processes at conditions of flow and temperature up to 400 kg/h and 673 K respectively. The centrifugal compressor aspires air from its surroundings which is then lead through the pipelines, passing through the hot-wire flow meter and through the electric heater. Finally, the air flow reaches the burner at conditions of mass and temperature desired. The burner can be coupled with different outside diameters, swirls, and injectors.

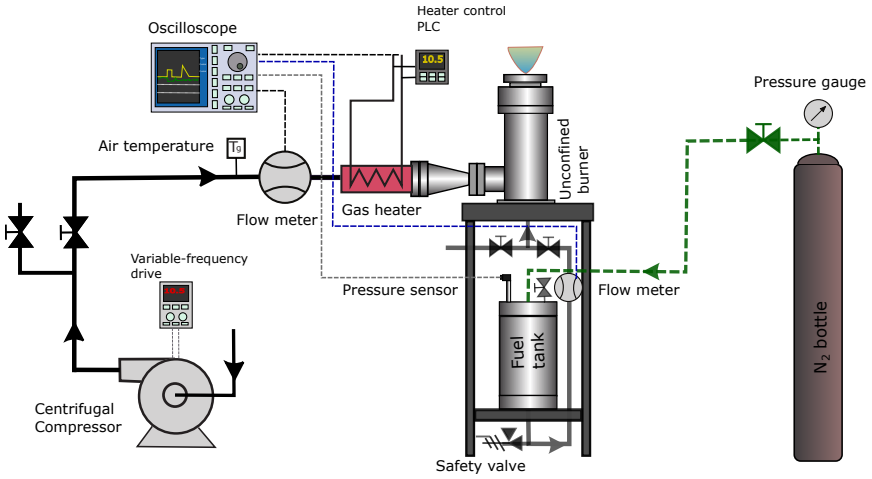


**Figure 1.** Global diagram of the high flow and temperature facility.

The injection system is formed principally by a pressurized vessel which can be pressurized up to 5 MPa through a nitrogen bottle. The vessel has multiple sensors and valves inputs connections ports allowing for different sensors to enter the tank (e.g., thermocouples, pressure sensor) and valves to fill it with the fluid. A safety valve has also been installed to prevent an over-pressure. An electronic Coriolis mass flow meter (Bronkhorst, CORI-FLOW) has been installed for accurate measurement fuel mass flow rate. Furthermore, two electro-valves were installed downstream from the injector to control the pass of the fluid through it, cut off the flow and avoid the dribble of the injector. Injector used to perform the experiment was a simplex pressure atomizer with a spray angle of 80° and a mass flow of 0.57 Kg/h at 1 MPa for calibration fluid (ISO 4113).

The continuous flow burner has full optical accesses allowing direct visualization of the spray. The design is modular and can be easily rearranged to simulate various configurations both geometrical and air surrounding properties. The simplex injector is mounted in such manner that the whole spray can be registered from the nozzle tip. Furthermore, a cross-section of insulating material was utilized between the external housing and the internal flow duct to avoid the heat losses of the test chamber.

### *Optical Technique and Setup*

#### *Microscopic diffused back-illumination technique*

The principle of this technique is based in the one used for study spray liquid penetration and arises from the consideration of the liquid phase as the dark silhouette of the spray when the background is illuminated with a

diffuse beam light. MDBI technique was applied to study the liquid spray characteristics of the injection process both size droplet and displacement of droplets (droplet velocity). This optical setup is composed mainly of a light-emitting diode (LED) as a light source and a high-speed camera, on opposing sides of the spray jet in a line-of-sight arrangement. A fast white LED was selected for this investigation which is capable of short (10 ns), high-power pulses of light at high repetition rates.

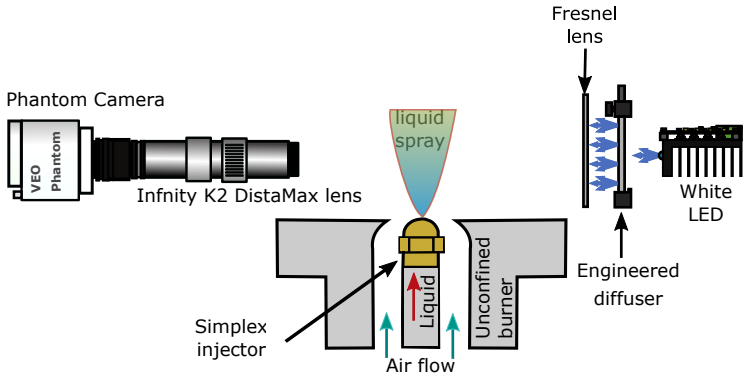


**Figure 2.** Scheme of the optical set up used for Microscopic diffused back-illumination.

A LED pulse duration was set to 300 ns as a compromise between illumination intensity and speed sufficient to "freeze" the droplet within the section of the spray jet. The light from the LED passes through an engineered diffuser (divergence angle of 20° and 100 mm of the diameter) which creates a surface that is diffusely illuminated, and then through a Fresnel lens, it is amplified and reproduced in the study zone where the spray is located. The camera captures the light that is not blocked by the spray (e.g., ligaments, and droplets) and thus, rendering the liquid phase of the spray as a shadow or dark pixels in the images. The use of a high-speed pulsing LED as a light source make this optical setup the best option for liquid phase visualization of the spray. MDBI allows the capture of images sharper than continuous light sources, reducing the actual timing and spatial uncertainties of the captured image [12, 13].

A high-speed camera (Phantom VEO 640) was located on the other side of the sprays. The recorder speed of the camera was set at 1,000 frames per second (fps). For this work, the camera was equipped with an Infinity K2 DistaMax lens to amplify the spray formation region near to the nozzle outlet and thus, identified its evolution. The exposure time of the camera was set in a PIV mode with the goal to get the highest intensity period of the LED illumination and minimize the time gap between consecutive frames, the illumination system pulse duration determines the exposure timescale (300 ns). A schema of the optical setup for the microscopic diffused back-illumination technique is presented in Figure 2.

Infinity K2 DistaMax lens provided a spatial resolution of the images of 5.6 µm per pixel, and therefore, the visualization and tracking of the liquid spray droplets by acquiring images, with a depth of field of 0.3 mm. Some details of the optical setup are presented in Table 1.

**Table 1.** Details of the optical setup for the employed techniques.

| | **Microscopic diffused back-illumination** |
|---|---|
| Camera | Phantom VEO 640 |
| LED pulse duration | 300 ns |
| Lens | K2 DistaMax |
| Frame rate | 1000 fps. |
| Resolution | 2560x1600 |
| Shutter time | PIV mode |
| Pixels/mm ratio | 177.5 |
| Repetitions | 248 |

Microscopic diffused back-illumination method consists of a record of successive frames with a background illumination controlled by pulses. The camera was set in PIV mode in order to obtain a high refresh rate of the recorded pixels and to allow a minimum temporal gap between the end of the one frame and the start of the next one. Considering frame A and Frame B, a LED pulse is sent at the end of the frame A and the other one at the beginning of the frame B, in order to get two frozen instants of the droplets with a quite short time between them (2.5 µs). The camera is responsible for sending the trigger to a BNC-pulse generator and then to the fast-LED with the configuration tuned as presented in Figure 3.

***Image processing***

To process the data obtained through the MDBI technique, an algorithm was implemented with the goal to determine the microscopic properties of the spray at the central plane near to the nozzle exit. In captures can be accurately identified and tracked particles larger than 17 µm, while the small particles were not treated. The relatively high

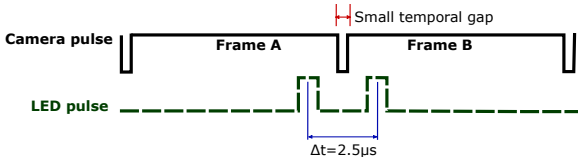


**Figure 3.** Scheme of pulses from the camera and the LED.

particle size captured was limited by the optical setup and was optimized to favor the largest field of view and record a reasonable spray length. The method employed is described below:

***Droplet size determination***

For the near field visualization, the general configuration presented in Figure 2 was used. The magnification provided by K2 DistaMax microscopic lens the droplets of the liquid spray can be seen and measured, allowing the determination of their diameter. The capture window was realized at the first millimeters from the nozzle tip, with 9 mm height and 14 mm width (see Figure 4.a). The processing methodology implemented to determine the microscopic spray characteristics is the following:

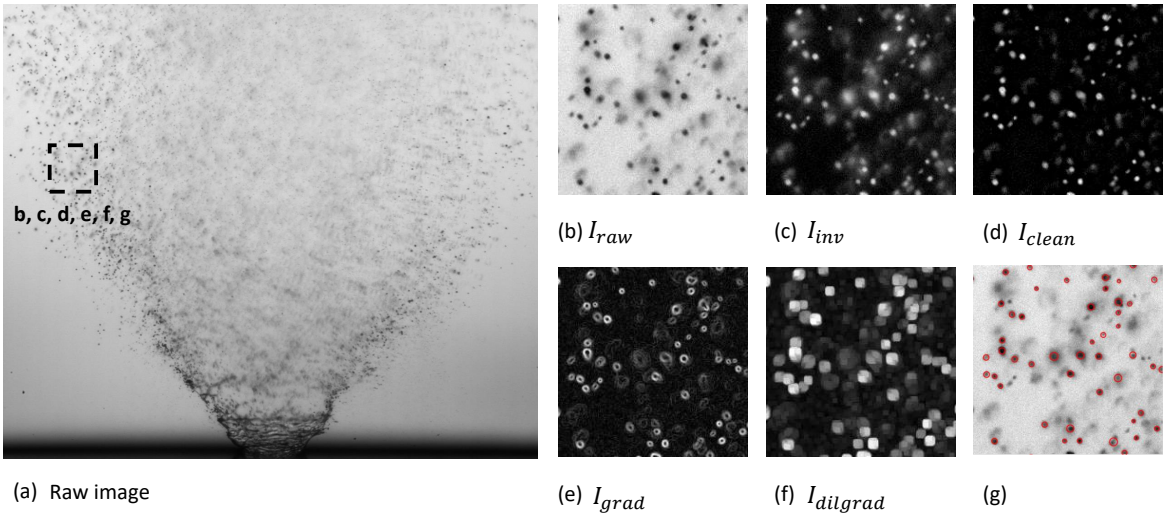


**Figure 4.** a) Raw image of the n-Dodecane spray jet at an injection pressure of 1.1 MPa, air flow of 28.5 kg/h and air temperatures of 328 K using MDBI technique, the dashed rectangle in the figure indicates the location of the next images, only to appreciate easily the procedure followed. b) Section of the raw image. c) Image with background subtraction and inverting of the pixels. d) Smoothing background subtraction. e) The gradient for each particle was calculated. f) Dilate in order to move the maximum intensity of the gradient. g) Particles that overcome the thresholds set.

- Background subtraction: An arithmetic subtraction was made of the spray images with its corresponding background ($I_{inv} = I_0 - I_{raw}$) to remove both reflections and background objects that could generate bad estimations of the spray. Moreover, to obtained white particles, as shown in Figure 4.c. The backgrounds were determined as an average of the images captured ($I_0$) before the start of injection for each LED position with respect to the camera signal (a slight difference intensity was noted between consecutive frames).
- Smoothing background subtraction: A rolling average was applied to the resulting images from the previous step ($I_{inv}$), obtaining smooth images ($I_{smooth}$). Next, a subtraction was made ($I_{clean} = I_{inv} - I_{smooth}$) to filter out the blurred areas which have a low frequency and thus highlight higher frequencies particles (Figure 4.d).
- Gradient: A gradient estimation was made for each particle ($I_{grad}$) to identify the ones located at the middle plane of the spray jet, i.e., focused particles. High gradients represent particles defined and focused, as shown in Figure 4.e. Additionally, a dilate function was used to move the maximum intensity of the gradient to the particle center ($I_{dilgrad}$), as presented in Figure 4.f.
- Locate: A method was implemented to select both, the valid and focused particles because of some of the features are clearly wrong. They are fleeting peaks in brightness that are not actually particles. As a result, the image's information $I_{inv}$, $I_{clean}$ and $I_{dilgrad}$ and set thresholds, the "good" particles located at the study plane were determined, extracting their coordinates through the determination of the local maximum for each one (Figure 4.g).
- Characterization: Finally, after to distinguishing real particles from invalid ones with the criteria implemented. The relevant information for each particle was extracted from the intensity properties, e. g., particle size and mass center coordinates.

Figure 4.a shows that droplets are injected from the atomizer under a cone with an 80 degrees opening, following a direction that will force them to suddenly interact with the air co-flow. The central region contains a very low quantity of small droplets due to the centrifugal movement imposed by the swirling liquid injection inside the atomizer. An interesting fact that can be seen is that most of the droplets are spherical, however, there are others that are ligaments rather than spherical in shape. This observation was also previously reported [17], where they concluded that the droplet diameter values obtained with Back-light imaging and Phase-Doppler Anemometry are in good agreement, suggesting that Back-light could be a suitable option for droplet size determination. Furthermore, it is important to highlight that properties reported previously have been obtained with sub-pixel accuracy, leading in results with quiet precision. A comprehensive approach of droplet visualization and image processing can be found in [13, 18].

***Tracking of droplets***

This processing methodology is a continuation to the one used to determine droplet size, focusing in this case in the trajectory of each particle identified in the previous section. To determine the tracking of the particles must be added this step to previous ones:

- Link features into particle trajectories: From the previous steps, the particles have been located in each frame. Next, the particles will be tracking from frame to frame, giving each one a number for identification. First, a maximum displacement must specify (the farthest a particle can travel between the pair of frames). However, the value selected should be reasonable because a large value slows computation time considerably. For this study, 8 pixels is a reasonable value.

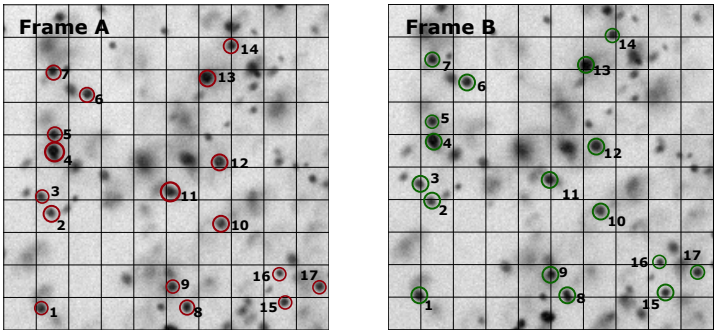


**Figure 5.** Location of the particles and number for identification for n-Dodecane droplets at an injection pressure of 1.1 MPa, air flow of 28.5 kg/h and air temperatures of 328 K using MDBI technique. Left: Frame A before the capturing ending. Right: Frame B after the capturing starting (time step between frames = 2.5 $\mu$s).

Figure 5 shows the displacement for each particulate. It is also important to note that the darker regions or spots captured in the pictures are not necessarily liquid droplets.

***Test conditions***

The experiments were performed using a simplex hollow cone injector commercially available. The liquids used were n-Heptane, n-Dodecane, and n-Hexadecane. Fuel properties are presented in Table 2.

**Table 2.** Fluid properties.

| Properties | n-Heptane | n-Dodecane | n-Hexadecane |
|---|---|---|---|
| Formula | C7H16 | C12H26 | C16H34 |
| Density [Kg/m$^3$] | 680$^a$ | 750$^a$ | 770 $^a$ |
| Viscosity [mPa·s] | 0.376$^b$ | 1.34$^b$ | 2.5$^b$ |
| Surface tension [mN/m] | 20.14$^a$ | 25.35$^a$ | 27.47$^a$ |

$^a$ At 293 K
$^b$ At 300 K

Experiments were carried out in accordance with the conditions summarized in the test matrix presented in Table 3. For each condition, 248 repetitions were taken.

**Table 3.** Test conditions matrix.

| Parameter | Value | Unit |
|---|---|---|
| Injection Pressure | 1.1 and 1.7 | [MPa] |
| Gas Mass Flow | 28.5 | [kg/h] |
| Gas Temperature | 328 | [K] |
| Oulet air diameter | 21 | [mm] |

**Results and discussion**

Figure 6-Left shows size droplet distribution for n-Dodecane spray jet at the nozzle exit. Two pressure levels were tested at fixed operating conditions (air temperature of 328 K and air flow of 28.5 kg/h), during the stabilized zone of the injection event. A wide range of diameter size distribution was captured. Nevertheless, the minimum diameter able to compute was about 17 $\mu$m due to the optical zoom restriction and pix/mm relation. Results reported by other authors for analogous conditions [17], mentioning that the number of droplets below 15 $\mu$m size are quite low. At the studied zone, the pressure has a significant influence on the droplet size distribution. Regarding Figure 6-Left is notorious that the higher pressure produces finer droplet size distribution. Meanwhile, the lowest pressure tends to form larger droplets and heterogeneous distribution, suggesting an initial worst atomization process. The overall values obtained in this work are in the same order of magnitude than those found by other authors [8, 11, 17, 19]. The higher the injection pressure promotes better atomization, producing narrower droplet diameter distribution and shifted to the left.

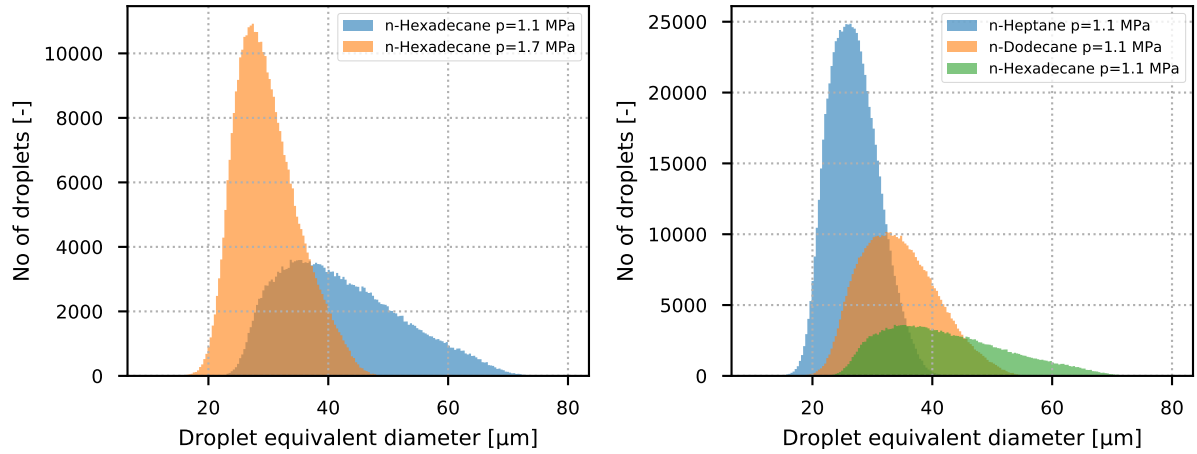


**Figure 6.** Left: Size droplet distribution for a spray of n-Hexadecane at two values of injection pressure and at fixed operating conditions (air temperature: 328 K and air mass flow: 28.5 kg/h. Right: Size droplet distribution for a spray of n-Dodecane, n-Heptanea and n-Hexadecane at fixed conditions (injection pressure: 1.1 MPa, air temperature: 328 K and air flow: 28.5 kg/h)

Figure 6-Right represents the size droplet distributions for n-Heptane, n-Dodecane, and n-Hexadecane fluids at fixed operating conditions presented in Table 3 and an injection pressure of 1.1 MPa. Hexadecane droplets resulting from the liquid jet breakup present a heterogeneous distribution, with droplet sizes ranging from 25 to 70 $\mu$m. Characteristics of the spray are widely influenced by the physical properties of the fluid such as density, viscosity, and surface tension [20]. In Table 2, n-Hexadecane presents the highest values for the liquid properties mentioned previously, n-Dodecane and n-Heptane present medium and low values respectively. Therefore, n-Heptane present a narrower ranging droplet diameter distributions and lower droplets sizes. Surface tension is important in atomization because it represents the force that resists the formation of new surface area. Furthermore, the viscosity is also importance stems from the fact that it affects not only the drop size distributions in the spray but also the nozzle flow rate and sprays pattern [1]. However, the density has been reported to cause a lower effect on the atomization performance [20, 21].

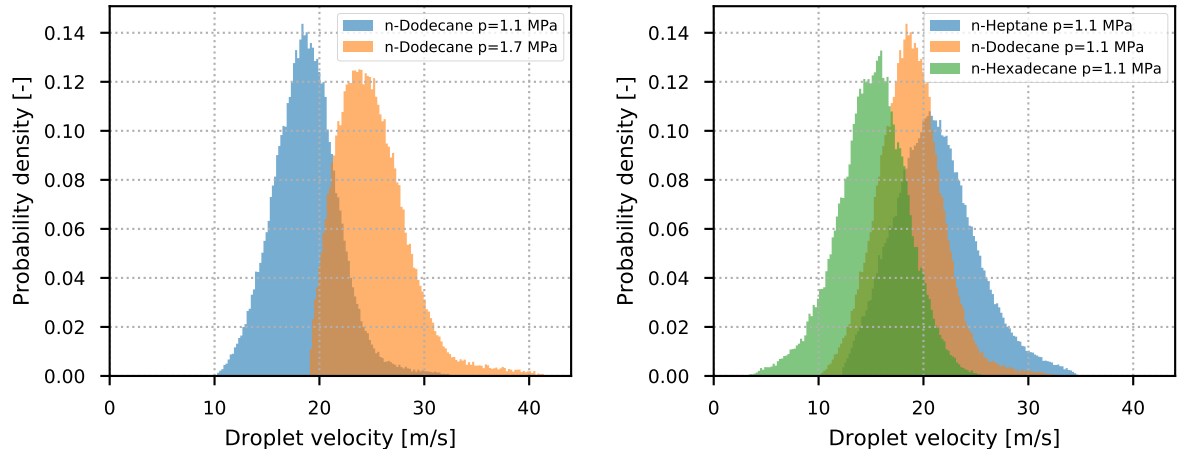


**Figure 7.** Left: Velocity droplet distribution for a spray of n-Dodecane at two values of injection pressure (1.1 MPa and 1.7 MPa) and at fixed operating conditions (air temperature: 328 K and air mass flow: 28.5 kg/h). Right: Velocity droplet distribution for a spray of n-Dodecane, n-Heptane and n-Hexadecane at fixed conditions (injection pressure: 1.1 MPa, air temperature: 328 K and air mass flow: 28.5 kg/h)

Figure 7-Left shows velocity droplet distribution for n-Dodecane spray jet, performing two injection pressure levels at fixed operating conditions presented in Table 3. To calculate the droplets velocity, the image processing methodology explained previously was used. In Figure 7-Left, note how the injection pressure has a significant influence on the droplet velocity. Lower pressure slows down the flow and decreases the breakup intensity, thus leading to larger structures [13]. Payri et al. [12] attributed this behavior to the variation of the momentum with a variation of the injection pressure. The results obtained for velocity are in good agreement with the ones found in other studies [1, 3, 11, 17]. The results found here support the processing methodology used in this work. Therefore, the methodology proposed is a viable alternative to measuring droplet velocity.

All experiments were performed for n-Heptane, n-Dodecane, and n-Hexadecane. Figure 7-Right shows how the properties of fluid have a noteworthy influence on the droplet velocity distribution. Measures were carried out at fixed conditions of the air surrounding, as shown in Table 3, and the value of the injection pressure was set to $1.1\,\mathrm{MPa}$. Regarding Figure 7-Right and Figure 6-Right, note how the n-Heptane spray presents smaller size droplet and thus higher velocity values. On the contrary, n-Hexadecane presents an opposite behavior, suggesting an initial worst atomization process, resulting in a higher size and lower velocity of the droplets due to the physical properties.

The droplet velocity is found to be inversely proportional to the viscosity of the fluid, Presser et al. [1] reported that this trend is to be expected since the droplet size and velocity have a direct relationship, for a given initial droplet momentum. Furthermore, the observations found here coincide to the results previously reported by Lefebvre [20]. To summarize, the droplet velocity is influenced by two phenomena: the Stokes number (small droplets are strongly accelerated by the co-flow while big droplets continue flying at smaller velocities until farther downstream) and the outlet velocity of the fluid from the injector.

**Conclusions**

This work presents an experimental methodology to analyze the microscopic characteristics of the spray at a middle cross-section and near to nozzle exit through Microscopic diffused back-illumination technique. The experiments were performed for three different fuels in a new test rig designed to study the atomization processes. From the findings, it is possible to conclude:

- Droplet size and velocity distributions have been obtained in pressure-atomized sprays for three different liquids (n-Heptane, n-Dodecane, and n-Hexadecane) from the pressure-swirl atomizer. The experiments showed that the fluid properties play an important role in the microscopic properties. Viscosity appears to have a significant effect on the droplet mean size and velocity. Fluid with higher viscosity (n-Hexadecane) generates larger droplets which tend to have lower velocities.
- The results show that the increase in the injection pressure improves the atomization process, delivering droplets with a smaller diameter as the pressure rises. Moreover, the regions further away from the injector exit registered a smaller diameter. Values of droplet size and velocity are in concordance with other studies, which investigated hollow-cone pressure-atomized sprays for different fluids. The data gathered provides a basic comprehension of the spray atomization process, as well as specific quantification useful for boundary conditions for CFD multiphase spray models.
- Future works will be done using the microscopic setup in order to explore more geometrical configuration, air surrounding conditions, and injection pressures. Additionally, a validation of the results obtained previously will be done using the PDA technique.

**Acknowledgements**

The author Santiago Cardona thanks the Universitat Politècnica de València for his predoctoral contract (FPI-2016-S1), which is included within the framework of Programa de Apoyo para la Investigación y Desarrollo (PAID-01-2016). We would like to thank María Del Carmen Sancho Fornes for the help during the measurement campaign. Part of the materials used in this work has been funded by the Generalitat Valenciana within the program “Subvencions per a la promoció i dinamització dels parcs científics” (PPC/2018/042).

**Nomenclature**

| | | | |
|---|---|---|---|
| fps | Frames per second | MDBI | Microscopic diffused back illumination |
| GRT | Global rainbow refractometry Technique | PDA | Phase Doppler Anemometry |
| LED | Light-emitting diode | PDI | Phase Doppler interferometry |
| LDV | Laser Doppler velocimetry | PIV | Particle image velocimetry |

**References**

[1] C. Presser, A. Gupta, C. Avedisian, and H. Semerjian, “Fuel property effects on the structure of spray flames,” *Symposium (International) on Combustion*, vol. 23, no. 1, pp. 1361–1367, jan 1991. [Online]. Available: https://www.sciencedirect.com/science/article/pii/S0082078406804017

[2] C. Edwards and R. Rudoff, “Structure of a swirl-stabilized spray flame by imaging, laser doppler velocimetry,

and phase doppler anemometry," *Symposium (International) on Combustion*, vol. 23, no. 1, pp. 1353–1359, jan 1991. [Online]. Available: https://www.sciencedirect.com/science/article/pii/S0082078406804005

[3] Mcdonell. G., M. Adachi, and G. S. Samuelsen, "Structure of Reacting and Non-Reacting Swirling Air-Assisted Sprays," *Combustion Science and Technology*, vol. 82, no. 1-6, pp. 225–248, mar 1992. [Online]. Available: http://www.tandfonline.com/doi/abs/10.1080/00102209208951821

[4] A. Cessou and D. Stepowski, "Planar laser induced fluorescence measurement of [OH] in the stabilization stage of a spray jet flame," *Combustion Science and Technology*, vol. 118, no. 4-6, pp. 361–381, 1996.

[5] J. A. Friedman and M. Renksizbulut, "Investigating a Methanol Spray Flame Interacting With an Annular Air Jet Using Phase-Doppler Interferometry and Planar Laser-Induced Fluorescence," *Combustion and Flame*, vol. 2180, no. 98, 1999.

[6] S. K. Marley, E. J. Welle, K. M. Lyons, and W. L. Roberts, "Effects of leading edge entrainment on the double flame structure in lifted ethanol spray flames," *Experimental Thermal and Fluid Science*, vol. 29, no. 1, pp. 23–31, 2004.

[7] H. Correia Rodrigues, M. J. Tummers, E. H. van Veen, and D. J. Roekaerts, "Effects of coflow temperature and composition on ethanol spray flames in hot-diluted coflow," *International Journal of Heat and Fluid Flow*, vol. 51, no. x, pp. 309–323, 2015. [Online]. Available: http://dx.doi.org/10.1016/j.ijheatfluidflow.2014.10.006

[8] A. Verdier, J. Marrero Santiago, A. Vandel, G. Godard, G. Cabot, and B. Renou, "Local extinction mechanisms analysis of spray jet flame using high speed diagnostics," *Combustion and Flame*, vol. 193, pp. 440–452, 2018. [Online]. Available: https://doi.org/10.1016/j.combustflame.2018.03.032

[9] I. Düwel, H. W. Ge, H. Kronemayer, R. Dibble, E. Gutheil, C. Schulz, and J. Wolfrum, "Experimental and numerical characterization of a turbulent spray flame," *Proceedings of the Combustion Institute*, vol. 31 II, no. 2, pp. 2247–2255, 2007. [Online]. Available: http://dx.doi.org/10.1016/j.proci.2016.06.039

[10] A. Verdier, J. Marrero Santiago, A. Vandel, S. Saengkaew, G. Cabot, G. Grehan, and B. Renou, "Experimental study of local flame structures and fuel droplet properties of a spray jet flame," *Proceedings of the Combustion Institute*, vol. 36, no. 2, pp. 2595–2602, 2017.

[11] J. Marrero Santiago, A. Verdier, A. Vandel, G. Godard, G. Cabot, and B. Renou, "Spray ignition and local flow properties in a swirled confined spray-jet burner: experimental analysis," in *Proceedings ILASS–Europe 2017. 28th Conference on Liquid Atomization and Spray Systems*. Valencia: Universitat Politècnica València, sep 2017.

[12] R. Payri, J. Gimeno, G. Bracho, and A. Moreno, "Spray characterization of the Urea-Water Solution ( UWS ) injected in a hot air stream analogous to SCR system operating conditions ." *WCX SAE World Congress Experience*, no. 2019-01-0738, pp. 1–9, 2019.

[13] J. Manin, M. Bardi, L. M. Pickett, R. N. Dahms, and J. C. Oefelein, "Microscopic investigation of the atomization and mixing processes of diesel sprays injected into high pressure and temperature environments," *Fuel*, vol. 134, pp. 531–543, 2014.

[14] J. Gimeno, P. Martí-Aldaraví, M. Carreres, and J. E. Peraza, "Effect of the nozzle holder on injected fuel temperature for experimental test rigs and its influence on diesel sprays," *International Journal of Engine Research*, vol. 19, no. 3, pp. 374–389, mar 2018.

[15] R. Payri, J. Gimeno, S. Cardona, and S. Ayyapureddi, "Measurement of Soot Concentration in a Prototype Multi- Hole Diesel Injector by High-Speed Color Diffused Back Illumination Technique," in *SAE Technical Paper 2017-01-2255*, 2017.

[16] C. Chen, Y. Yang, X. Wang, and W. Tang, "Effect of geometric and operating parameters on the spray characteristics of an open-end swirl injector," *Proceedings of the Institution of Mechanical Engineers, Part G: Journal of Aerospace Engineering*, vol. 0, no. 0, pp. 1–11, 2019.

[17] A. Verdier, "Experimental study of dilute spray combustion," Ph.D. dissertation, Normandie Université, 2018.

[18] J.-B. Blaisot and J. Yon, "Droplet size and morphology characterization for dense sprays by image processing: application to the Diesel spray," *Experiments in Fluids*, vol. 39, no. 6, pp. 977–994, 2005.

[19] C. K. Law, "Recent advances in droplet vaporization and combustion," *Progress in Energy and Combustion Science*, vol. 8, no. 3, pp. 171–201, 1982.

[20] A. H. Lefebvre and V. G. McDonell, *Atomization and Sprays*, C. Press, Ed. Taylor & Francis Group, 6000 Broken Sound Parkway NW, Suite 300, Boca Raton, FL 33487-2742: CRC Press, apr 2017. [Online]. Available: https://www.taylorfrancis.com/books/9781498736268

[21] L. S. Christensen and S. L. Steely, "Monodisperse atomizers for agricultural aviation applications," NACA, Tech. Rep., 1980.